REPORT DOCUMENTATION PAGE

Form Approved
OMB No. 0704-0188

PLEASE DO NOT RETURN YOUR FORM TO THE ABOVE ORGANIZATION.

1. REPORT DATE *(DD-MM-YYYY)*	2. REPORT TYPE	3. DATES COVERED *(From - To)*
10-26-2004	Journal Article	

4. TITLE AND SUBTITLE

A Numerical Simulation of the East Asian Seas in March 2002: Effect of Vertical Grid Choice

5a. CONTRACT NUMBER

5b. GRANT NUMBER

5c. PROGRAM ELEMENT NUMBER

0602435N

6. AUTHOR(S)

Andrea C. Mask, Ruth H. Preller

5d. PROJECT NUMBER

5e. TASK NUMBER

5f. WORK UNIT NUMBER

73-6646-04-5

7. PERFORMING ORGANIZATION NAME(S) AND ADDRESS(ES)

Naval Research Laboratory
Oceanography Division
Stennis Space Center, MS 39529-5004

8. PERFORMING ORGANIZATION REPORT NUMBER

NRL/JA/7300-04-5019

9. SPONSORING/MONITORING AGENCY NAME(S) AND ADDRESS(ES)

Office of Naval Research
800 N. Quincy St.
Arlington, VA 22217-5660

10. SPONSOR/MONITOR'S ACRONYM(S)

ONR

11. SPONSOR/MONITOR'S REPORT NUMBER(S)

12. DISTRIBUTION/AVAILABILITY STATEMENT

Approved for public release, distribution is unlimited.

13. SUPPLEMENTARY NOTES

14. ABSTRACT

The sensitivity of vertical grid choice in the hybrid Navy Coastal Ocean Model (NCOM) is discussed for the Yellow Sea, East Asian Sea, Japan/East Sea domain. In particular, the logarithmically stretched hybrid vertical profile used operationally at the Naval Research Laboratory is compared to six variations. The variations include a full z-level run, a full sigma coordinate run, and other hybrid constructs that modify the hybrid's transitions depth or the structure of the operational grid. The results are compared to each other and some limited observations in the framework of setting up a rapidly relocatable ocean model. The comparisons show that the operational vertical grid structure is a good first guess design for a rapidly relocatable ocean model.

15. SUBJECT TERMS

East China Sea; Yellow Sea; Japan/East Sea; Hybrid ocean models; NYCOM; MODAS

16. SECURITY CLASSIFICATION OF:			17. LIMITATION OF ABSTRACT	18. NUMBER OF PAGES	19a. NAME OF RESPONSIBLE PERSON
a. REPORT	b. ABSTRACT	c. THIS PAGE			Ruth H. Preller
Unclassified	Unclassified	Unclassified	UL	16	19b. TELEPHONE NUMBER *(Include area code)* 228-688-4670

Available online at www.sciencedirect.com
ScienceDirect
Ocean Modelling 18 (2007) 81–96
Ocean Modelling
www.elsevier.com/locate/ocemod

A numerical simulation of the East Asian Seas in March 2002: Effect of vertical grid choice

Andrea C. Mask *, Ruth H. Preller

Naval Research Laboratory, Code 7322, Stennis Space Center, MS 39529, USA

Received 10 January 2005; received in revised form 21 February 2007; accepted 22 February 2007
Available online 29 April 2007

Abstract

The sensitivity of vertical grid choice in the hybrid Navy Coastal Ocean Model (NCOM) is discussed for the Yellow Sea, East Asian Sea, Japan/East Sea domain. In particular, the logarithmically stretched hybrid vertical profile used operationally at the Naval Research Laboratory is compared to six variations. The variations include a full z-level run, a full sigma coordinate run, and other hybrid constructs that modify the hybrid's transitions depth or the structure of the operational grid. The results are compared to each other and some limited observations in the framework of setting up a rapidly relocatable ocean model. The comparisons show that the operational vertical grid structure is a good first guess design for a rapidly relocatable ocean model.

Keywords: East China Sea; Yellow Sea; Japan/East Sea; Hybrid ocean models; NCOM; MODAS

1. Introduction

Recent intercomparisons of ocean models, using different discretizations of the vertical coordinate such as the DYNAMO and DAMEE projects (as discussed by Haidvogel and Beckmann, 1999, pp. 267–275 and see also Willebrand et al., 2001; Chassignet et al., 2000), have underscored previous findings that isopycnal, terrain-following (sigma), and geopotential (z-level) vertical coordinates each have advantages and disadvantages in simulating the ocean environment. This has resulted in the attempt to design ocean models that use a hybrid vertical coordinate system to try to overcome the weaknesses and draw on the strengths of a particular coordinate. Examples of hybrid ocean models include the Navy Coastal Ocean Model (NCOM) developed at the Naval Research Laboratory (NRL) at Stennis Space Center (Martin, 2000), the Hybrid Coordinate Ocean Model (HYCOM) developed by RSMAS at the University of Miami (Bleck, 2002), and the generalized version of the Princeton Ocean Model (POM) developed at Princeton University (Mellor et al., 2002).

* Corresponding author. Present address: Naval Oceanographic Office, NP1, Stennis Space Center, MS 39522, USA. Tel.: +1 228 688 4088.
E-mail addresses: andrea.mask@navy.mil (A.C. Mask), preller@nrlssc.navy.mil (R.H. Preller).

1463-5003/$ - see front matter © 2007 Elsevier Ltd. All rights reserved.
doi:10.1016/j.ocemod.2007.02.007

One particular issue to be resolved in the use of ocean models with hybrid grids is given a particular topography what vertical grid construct produces the best results. This study attempts to evaluate the effect of the choice of vertical grid on a rapidly relocatable NCOM design. The rapidly relocatable NCOM's design purpose is the "on demand" setup of a new nested NCOM geographic area in the timeframe of a few hours or days instead of a few months. To accomplish this feat, grid design and forcing sources must be predetermined. The grid design includes a predetermined vertical grid structure which gives robust results over a variety of different topographies. To test this rapidly relocatable NCOM, an area including the Yellow Sea, East China Sea, and Japan/East Sea was chosen because of its limited size and varied topography and dynamics. Different designs of the rapidly relocatable NCOM vertical grid are set-up and then compared to each other and to some limited observations to determine the sensitivity of the design and which design best represents the circulation and density structure of the modeled area. Such vertical grid analyses have been made for the HYCOM (Halliwell, 2004) with a low-resolution, climatological Atlantic Ocean and for the POM (Mellor et al., 2002) with an idealized deep ocean basin.

The model setup used operationally at NRL and the vertical grid designs to be tested will be discussed in Section 2. In Section 3, the comparative results will be presented for each region of interest: the Yellow Sea, the East China Sea, and the Japan/East Sea. Section 4 discusses the need for using a 3D dynamic climatology in the operational NCOM setup. Finally, general conclusions will be drawn and overall statistics will be discussed in Section 5.

2. Model setup

The model used in this study is the Navy Coastal Ocean Model (NCOM) (Martin, 2000). This model is hydrostatic, Boussinesq, and incompressible and has been developed with a hybrid vertical coordinate which allows the user to specify a vertical grid of all sigma coordinates, all z-levels (with the exception of a free surface sigma layer), or a combination of the two with sigma layers near the surface and z-levels near the bottom. This configuration allows the use of sigma layers in shallow areas and z-levels in deep areas.

This model is currently being run operationally as a nowcast/ forecast system both as an 1/8° global ocean model (Barron et al., 2006) and as a 1/16° East Asian Seas model (EAS16) (http://www7320.nrlssc.navy.mil/EAS16_NFS/). Daily runs of these models mean there are readily available forcing fields and boundary conditions for rapidly relocatable runs. The EAS16 is used in this rapidly relocatable study for initialization and boundary conditions for a 1:1 horizontal coupling to a 1/16° Yellow Sea, East China Sea and Japan/East Sea region model (Fig. 1). The vertical grid structure of the coupled subdomain tested here is modified from the standard EAS16 vertical grid. The standard EAS16 vertical grid is the operational vertical grid also employed by the NCOM global model. The EAS16 nowcast/forecast system is currently being run with tides, but this study uses an older version of the model which was run only in nowcast mode with no tides from 30 December 2000 to 22 February 2003. In particular, the model time period for this study is March 2002.

The model used in this study (hereafter called YS16) is forced by the Navy Operational Global Atmospheric Prediction System (NOGAPS) (Hogan and Brody, 1993; Rosmond, 1992; Hogan and Rosmond, 1991) atmospheric fields and lateral boundary conditions which are regridded from the EAS16 model output. YS16 assimilates Modular Ocean Data Assimilation System (MODAS) dynamic climatology sea surface temperature (SST) and salinity (SSS) and a MODAS 3D temperature and salinity dynamic climatology product (Fox et al., 2002). The assimilation of the MODAS data is achieved through relaxation of the model values to the MODAS temperature and salinity analyses. The relaxation is weaker near the surface and stronger at depth. The NOGAPS forcing is identical for all the runs; the 3D MODAS and the lateral boundary conditions are linearly interpolated to the particular vertical grid for each case. The lateral boundary conditions use an advective scheme for the normal velocity, a zero gradient scheme for the tangential velocity, and the Orlanski radiation scheme for temperature and salinity. Following a rapidly relocatable framework, the YS16 forcing and assimilation are applied in the same manner as the NCOM global model and the EAS16 model that are run operationally.

There are seven different vertical grid configurations tested here (Table 1). All are similar to the EAS16 vertical grid in some way. The standard EAS16 vertical grid consists of 40 levels; the top 20 are sigma layers. It is logarithmically stretch with δz varying from 1 m at the surface to 800 m in the deep water. The transition

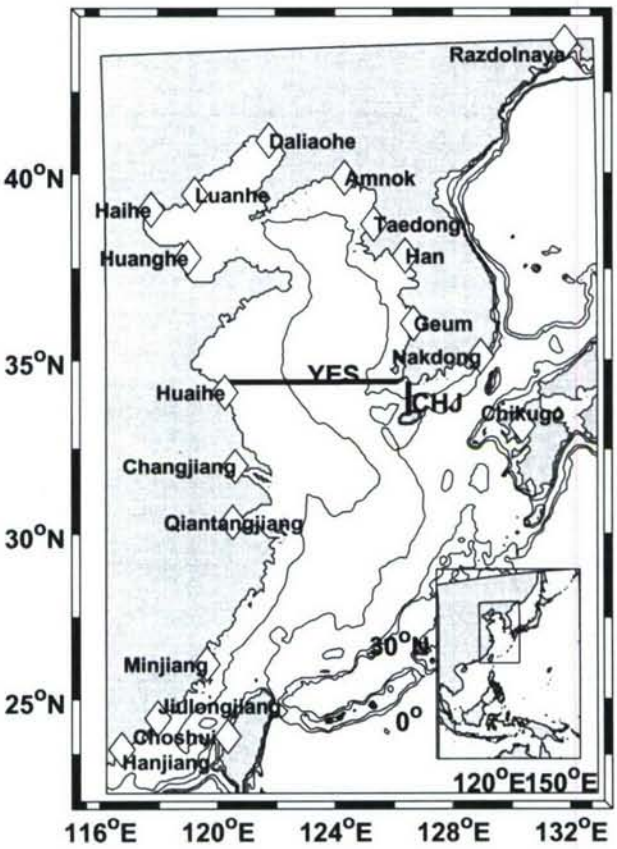

Fig. 1. YS16 domain with river locations and transport lines shown. Bathymetry contours are for 50, 100, 500, and 1000 m. EAS16 domain shown in inset with EAS16 domain location shown.

Table 1
YS16 vertical grid definitions

Run name	Number of z's	Number of Sigma's	Notes
YS16stnd	20	20	The operational NCOM vertical grid Transition depth at 137.87 m
zgrid	38	2	A full z-level case with a sigma free surface
sgrid	0	40	A full sigma coordinate case
hy15	25	15	Transition depth at 54.76 m
hy22	18	22	Transition depth at 197.36 m
botres	20	20	High bottom resolution on shelf
sufbotres	20	20	High surface and bottom resolution on shelf

depth from sigma coordinates to z-levels is 137.87 m. For the YS16 study region, the transition depth of the standard grid (YS16stnd) is approximately 80 m above the 200 m shelf break. A full sigma coordinate (sgrid) and a full z-level (zgrid) case follow the same logarithmic profile as the standard grid. Two additional hybrid cases also follow the logarithmic profile. The "hy15" case has fifteen sigma layers and a transition depth of 54.76 m, which is approximately half the maximum depth of the Yellow Sea. The "hy22" case has 22 sigma layers and a transition depth of 197.36 m, which is the z-level depth closest to the shelf break depth. The final two grids modify the log profile in order to increase the resolution near the bottom in the shelf region. The "botres" case flips the δz of the log-linear profile above the transition depth of 137.87 m such that there is a δz of 15 m at the surface and a δz of 1 m at 125 m depth. The "sufbotres" case is a mixture of the YS16stnd and the botres case such that there is high vertical resolution near the surface as in the log-linear profile down

to 63 m then the δz decreases back to 1 m at 125 m. In both the botres case and the sufbotres case, the vertical grid below the 137.87 m transition depth is the same as in the YS16stnd case.

The sgrid case uses different lateral boundary conditions than the rest of the runs. This case uses an Orlanski radiation scheme for the u- and v-velocities and an advective scheme for temperature and salinity. This is necessary to keep the run stable, but perhaps does not produce the best results. Only the original lateral boundary conditions, that were not stable, and the schemes used here were tested. The sgrid bathymetry has not been modified or smoothed to reduce potential pressure gradient errors. It was desired to keep the bathymetry the same for all runs because of the rapidly relocatable framework. Haidvogel and Beckmann (1999, p. 139) introduces a parameter $r = \Delta h/2h$ to determine if the bathymetry is smooth enough to use with sigma coordinate grids. They say that the value of r should not much more than 0.2. The maximum value of r for sgrid is 0.71, and 20% of the ocean points have r values larger than 0.2; therefore, smoothing the sgrid bathymetry could improve results in areas of steep topography, such as the shelf break regions.

3. Results

The YS16 study region was chosen in part because of its varied topographical areas. The Yellow Sea is very shallow with a maximum depth around 100 m, the East China Sea is a shelf break region, and the Japan/East Sea is very deep with a maximum depth over 3000 m within the study region. The variation in topography makes it difficult to design a vertical grid that performs well in all areas. The hybrid vertical coordinate helps in this situation, but determining the optimal transition depth and ratio of sigma coordinates to z-levels can be a challenge. For a rapidly relocatable system, it is desirable to have a robust vertical grid that performs well in a variety of topographical areas to ease the set-up configuration.

Next, each area is discussed separately to see if there are any definable trends in the results. Most of the discussion will be limited to the YS16stnd, zgrid, and sgrid cases as these are representative of the overall results.

3.1. Yellow Sea: shallow

For this study, the Yellow Sea (YS) is primarily confined to the sigma coordinate portion of the hybrid vertical grids. Between the surface and 100 m there are a maximum of 40 layers in the full sigma case and a minimum of 18 levels in the full z-level case. The z-level case has 11 levels in the upper 25 m. In March, the vertical temperature structure of the YS is strongly influenced by the East Asian monsoon whose northerly winds mix the basin. Therefore, one would expect different vertical grids to have a minimal effect during this time period. This is mostly true, but there are regions of the YS that appear sensitive to changes in the vertical grid. Two such regions are areas of river outflow and the Western Cheju do Front, which is located between the Korean Peninsula and the island of Cheju.

There are eleven modeled rivers flowing into the Yellow and Bohai Seas; the Geum and Han in South Korea, the Taedong and Amnok (Yalu) in North Korea, and the Qiantangjiang, Huaihe, Huanghe (Yellow), Haihe, Huanhe, Daliaohe, and Changjiang (Yangtze) rivers in China (Fig. 1). These rivers are forced with a monthly climatological temperature and outflow velocity defined at a single point with values at all depths. The outflow salinity is set to zero. The river outflow values are interpolated in time with the climatological value reached in the middle of a given month.

The modeled salinity is particularly sensitive to differences in the vertical grid for the river outflow regions (Fig. 2). Modification of the vertical grid adjusts the river front locations. This sensitivity has also been noticed by Hyatt and Signell (1999). In looking at a representative river, the Changjiang's salinity front location is highly variable from grid to grid. As compared to the YS16stnd case, the zgrid, hy15, hy22, and sufbotres case's variability is confined to the Changjiang's plume region, while the sgrid and botres cases' variability continues north along China's coast. The hy15 case appears to have the least amount of RMS difference in the Changjiang region as compared to the YS16stnd case. The variation in river plume front location is mainly the result of vertical grid induced differences in river outflow transport.

The Western Cheju do Front has a strong temperature gradient during March 2002. The YS16stnd (Fig. 3) shows a range of 10–14 °C across the front at the surface. This is consistent with the range of 10.5–14.5 °C

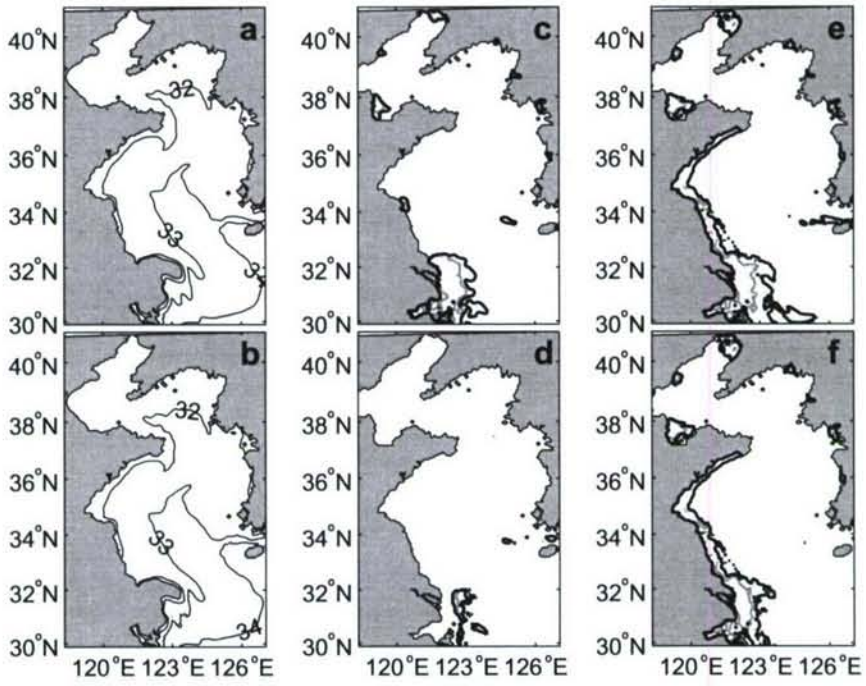

Fig. 2. Layer 1 (upper figures) and layer 10 (lower figures) salinity (a and b) for a sample day (31 March 2002) on the YS16stnd grid and the 0.2 (black) and 0.4 (gray) RMS difference over the length of model integration for the zgrid (c and d) and sgrid (e and f) as compared to the YS16stnd grid.

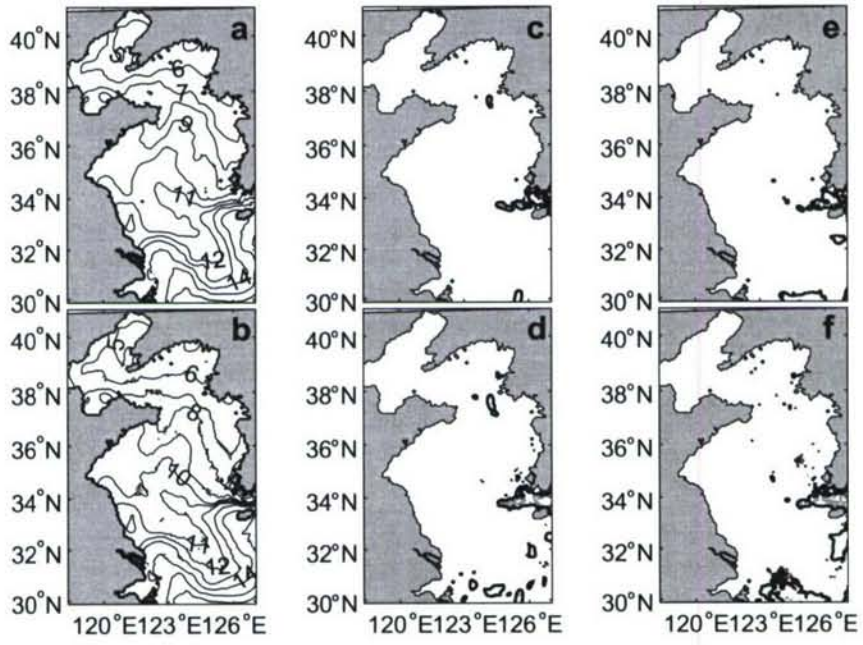

Fig. 3. Same as Fig. 2 except for temperature.

found in March of 1997 (Chang et al., 2000). The zgrid and sgrid have RMS differences of around 0.2 °C at the surface in this frontal region, and RMS differences of around 0.4 °C at level 10 (approximately mid-depth in the Yellow Sea). The hy15 case is most similar to the results of the zgrid and sgrid cases. The sufbotres case has

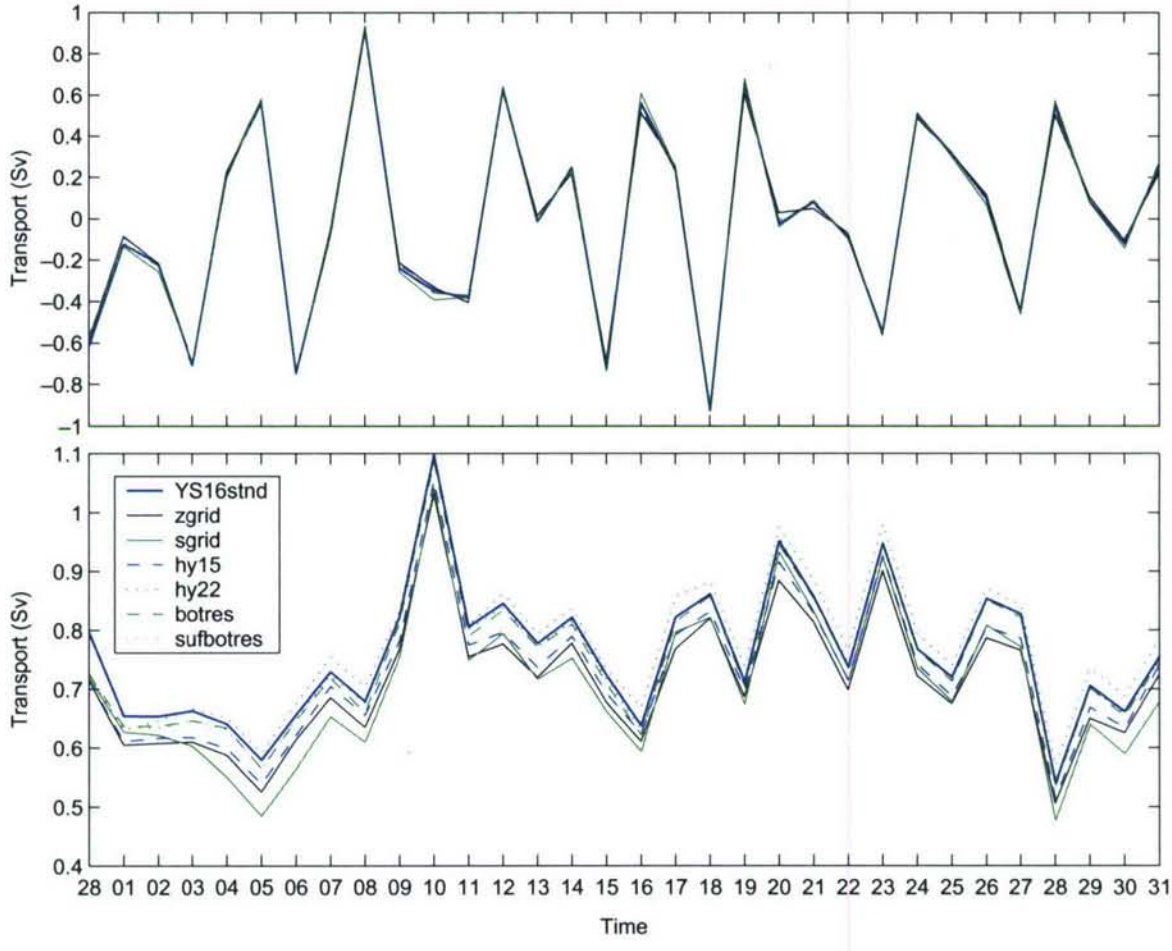

Fig. 4. Transport for YES line (upper) and the CHJ line (lower) for the seven cases.

similar patterns to the zgrid and sgrid cases, but the RMS difference is around 0.4 °C at the surface and around 0.2 °C at level 10. The hy22 case is most similar to the YS16stnd case with minimal differences at both levels. The botres case is the most dissimilar to the YS16stnd case not only in the Western Cheju do Front but in most of the coastal areas. This is because the upper-most layer is at a depth of 15 m.

The currents in the YS basin are very consistent between cases. The mean transport across the basin ranges from −0.0126 Sv for the zgrid and hy15 cases to −0.0144 Sv for the YS16stnd case (Fig. 4) which is a good comparison to the "essentially no transport" found by Candela et al. (1992) in January 1986. The Western Cheju do Front area has more variability between runs. Its mean transport ranges from 0.7048 Sv for the sgrid case to 0.7739 Sv for the hy22 case. This is larger than the observed transport of 0.45 Sv in March 1997 (Chang et al., 2000). The model produces a stronger current along the front than is observed in 1997.

It appears that in the shallow water of the YS that the hy15 and hy22 cases are the most similar to the YS16stnd case, yet because of the shallowness of the basin and the wind forcing, all the models produce similar circulation results. It is not clear which run best represents reality because there are no observations available in the YS during March 2002.

3.2. East China Sea: shelf break

The East China Sea (ECS) region is dominated by the Kuroshio, which enters the region to the east of Taiwan and exits south of Japan's Kyushu island. The Kuroshio flows along the shelf break, which is approximately the 200 m isobath. This region employs the full hybrid grid with depths down to 5500 m in the Pacific

Ocean region east of the Ryukyu island chain and depths of almost 2000 m west of the Ryukyu island chain. This region is also influenced by the lateral boundary conditions imposed on the southern and eastern boundaries.

Intercomparison of the grids through RMS differences of velocity as compared to the YS16stnd shows that most of the RMS difference is below the 5 cm/s level (Fig. 5). This is not true for the sgrid which shows large RMS difference in the Kuroshio region and along the boundaries. Much of the difference in the sgrid in the ECS could be the result of the steep topography that has not been smoothed to reduce horizontal pressure gradient errors. There also appears to be more boundary reflection in the sgrid case than any of the other cases, particularly in the Kuroshio inflow and outflow regions. This is probably the result of using Orlanski boundary conditions for the velocity components, which was necessary for the sgrid run to be stable. It should also be noted that full sigma grids are known to have stronger currents at depth than z-level grids produce (Haidvogel and Beckmann, 1999, pp. 267–275).

Comparison to some limited observations during this time period can give a different perspective of the model output. Two unique observational data sets are discussed for the ECS region. First, five XBT casts give a temperature comparison in the Kuroshio region south of Japan (Fig. 6). The XBT data were obtained from the Japan Oceanographic Data Center's (JODC) website (http://www.jodc.go.jp/). Another piece of observational data is a drifter track in the Kuroshio from the global drifter data set maintained by the Atlantic Oceanographic and Meteorological Laboratory (AOML).

The XBT data (Fig. 6) clearly show a mixed layer depth of approximately 25 m in all but one of the locations. This mixed layer is not present in the model data, except for the sgrid run on 13 March, whose mixed layer is deeper because of strong currents in the area produced by boundary reflection. Note that most of the model runs have identical profiles which should resemble the 3D MODAS product because the model temperature and salinity are relaxed to the MODAS fields (with a stronger relaxation at depth). The discrepancy between the model and the MODAS temperature is the result of a broad, rather stationary Kuroshio in MODAS as compared to the more variable modeled Kuroshio, and the lack of a mixed layer is the result of light winds in the NOGAPS forcing fields.

The drifter data (Fig. 7) has been interpolated to every 6 h using kriging by AOML. The velocities have then been corrected using NCEP reanalysis winds from UCAR using both the drogued data and undrogued data (Niiler, 2001; Hansen and Poulain, 1996). The drifter is drogued to 15 m depth, and the track enters the YS16 domain on 01 March 2002 with the first time step at hour 12. Only the portion of the track that corresponds to March 2002 is shown. A drifter track has been constructed from the 12-hourly model output for each of the runs. This is accomplished with a 4th-order Runga–Kutta method integrated to hourly time steps to propagate the solution forward 12 h. That 12 h solution is used as the new starting point and the solution is

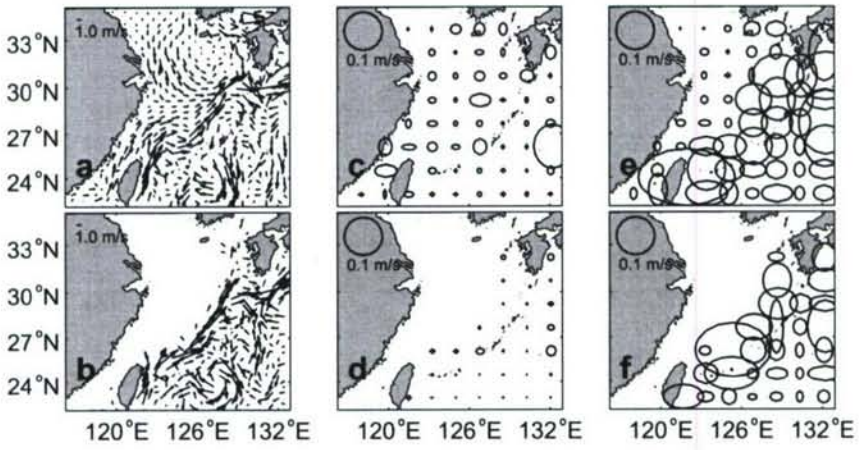

Fig. 5. Layer 1 (upper figures) and layer 20 (lower figures) velocity (a and b) for a sample day (31 March 2002) on the YS16stnd grid and ellipses of RMS velocity difference over the length of model integration for the zgrid (c and d) and sgrid (e and f) as compared to the YS16stnd grid.

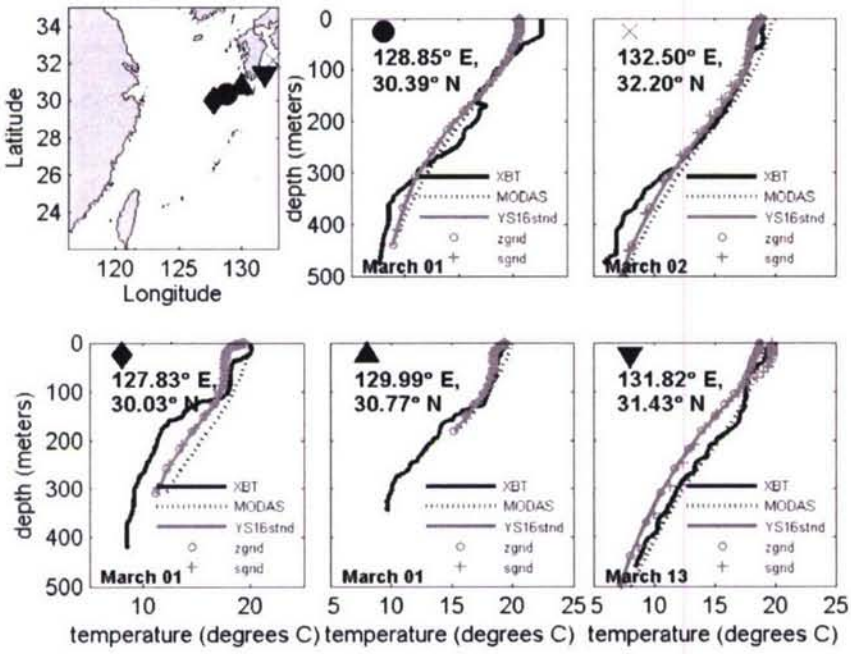

Fig. 6. Temperature profiles for three of the seven model runs, MODAS 3D, and XBT data which were obtained from the Japan Oceanographic Data Center's website (http://www.jodc.go.jp/). Profiles for the four models not shown overlay the YS16stnd case.

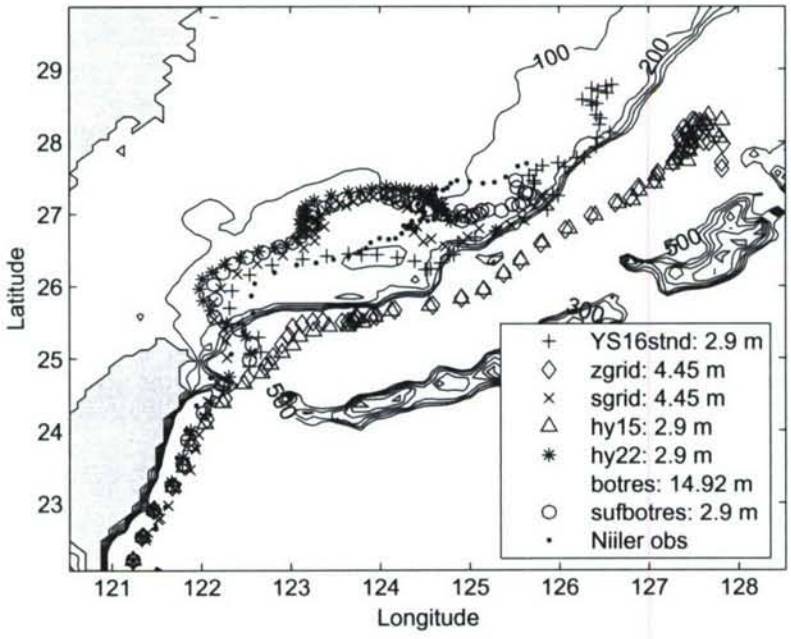

Fig. 7. Comparison between a Niiler drifter track and the calculated model drifter tracks. The model layer of best comparison is given in the legend. The bathymetry contours are at 100, 200, 300, 400, and 500 m.

propagated again. The model velocities at 15 m (layer 7) are too slow, which shows that the modeled Kuroshio is too weak; therefore, the layer whose result most resembles the observed track is plotted in Fig. 7, not the layer nearest to 15 m depth. This plotted layer is layer 3 (2.9 m) or 4 (4.45 m) for all the model runs except botres which is layer 1 (15 m). There are three model runs that do best at reproducing the observed drifter track; they are the YS16stnd run, the hy22 run, and the sufbotres run. The hy22 and sufbotres runs get

"caught" in a similar feature as the drifter at approximately 124.5°E, 26.75°N; however, this does not occur at the same moment in time because it takes about 5 days longer for the modeled drifters to arrive in the same location.

3.3. Japan/East Sea: deep

The portion of the Japan/East Sea contained in the YS16 region consists of the Tsushima (Ulleung) Basin and the western-most portions of the Japan Basin and Oki Spur. This subarea of the Japan/East Sea (JES) is dominated by the inflow of the Tsushima Warm Current (TWC) through the Tsushima Strait. The varied behavior of the TWC in the JES is discussed by Preller and Hogan (1998). For March 2002 the YS16 model produces a Nearshore Branch of the TWC along Japan, a meandering Offshore Branch, and an East Korean Warm Current along Korea that ends in an eddy centered at 130°E, 38.25°N (Fig. 8). This eddy is the [Kn] warm eddy discussed by Isoda and Saitoh (1993).

The RMS difference (Fig. 8) between YS16stnd and the other model runs show very small velocity differences except in the Tsushima Strait; however, the sgrid has large RMS differences because of weaker velocities in the interior and velocities flowing southward instead of northward on the narrow shelf as compared to the YS16stnd run.

There are some limited observations in the JES during March 2002 for which a comparison to the model results can be made. In particular, there are several temperature and salinity profiles supplied by PALACE floats in the JES (Figs. 9 and 10). These data were supplied by the Naval Oceanographic Office's (NAVOCEANO) Master Oceanographic Observation Data Set (MOODS; Teague et al., 1990). The observations can be broken into three distinct surface water mass regions of the Tsushima Warm Water; the Tsushima Warm Current region (TWC), the East Korean Warm Current region (EKWC), and a general Tsushima Warm Water region (TWW). The TWW region is identified by water above 150 m of high temperature (>5 °C) and high salinity (>34.1) (Preller and Hogan, 1998).

There are two observational locations of general TWW water; the circle on 05 March 2002 and the plus sign on 26 March 2002. Both of these points are located just south of the Subpolar Front, which is located

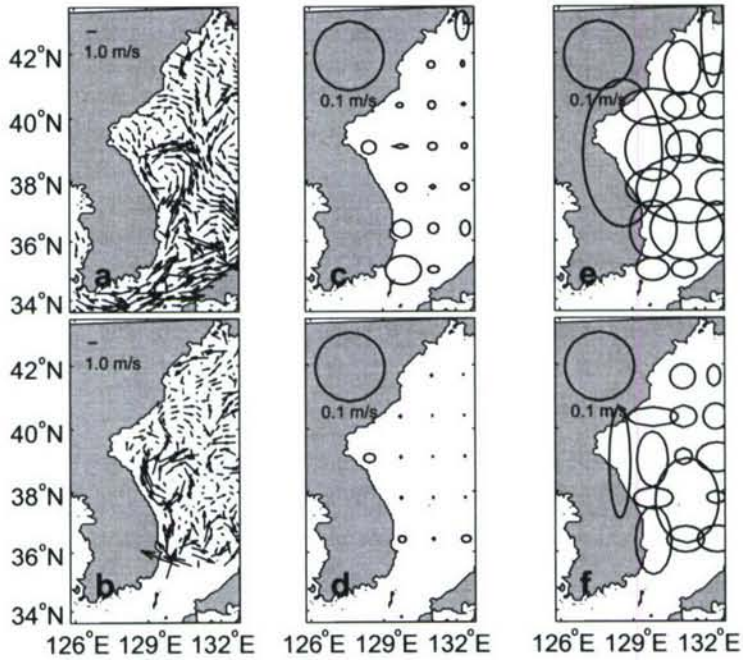

Fig. 8. The average velocity of (a) layer 1 and (b) layer 20 for March 2002 on the YS16stnd grid and ellipses of RMS velocity difference over the length of model integration for the zgrid (c and d) and sgrid (e and f) as compared to the standard grid for the same layers.

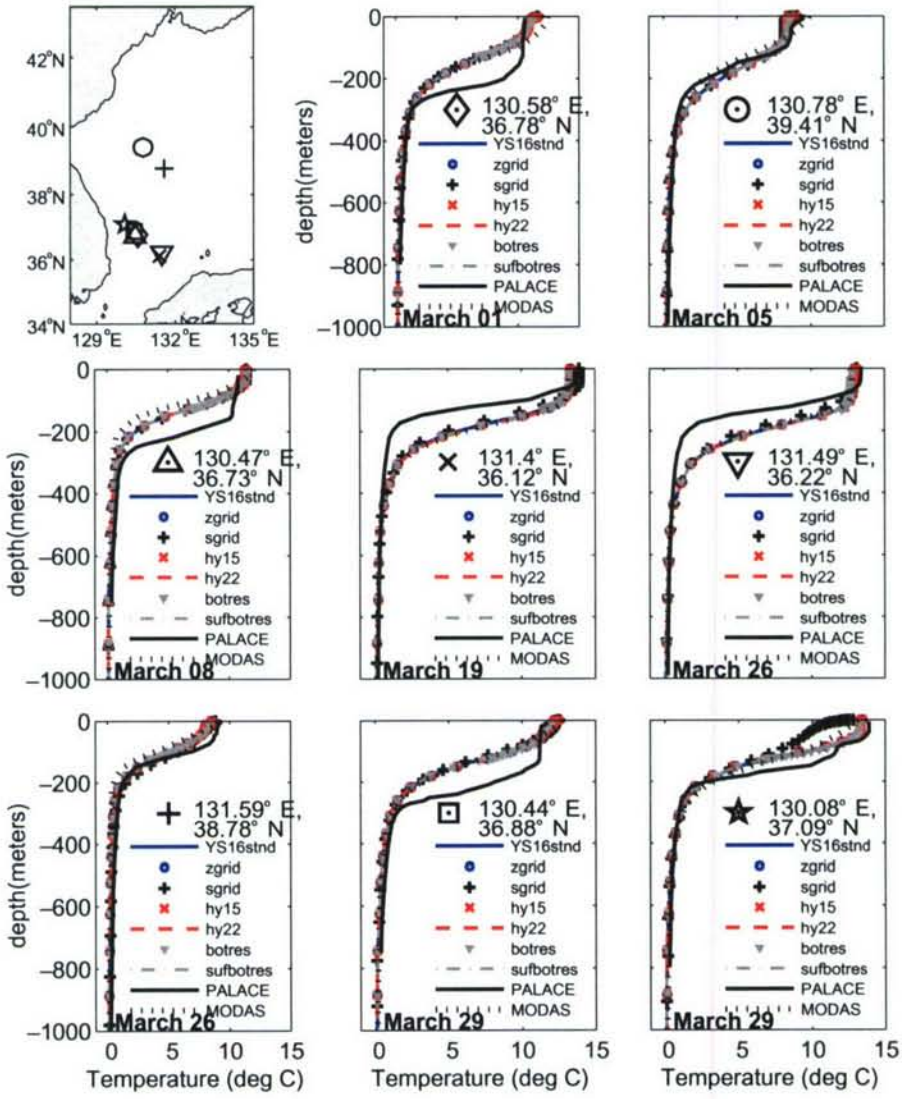

Fig. 9. Temperature (°C) profiles for the seven model runs, MODAS 3D, and PALACE float data.

approximately along 41°N latitude (not shown) for the model runs. The model temperature profiles approximately match the observations in this region as does the salinity for 05 March 2002, but the salinity for 26 March 2002 does not match the observations even though the MODAS forcing shows higher salinity in this location. The MODAS has a weak [Kn] eddy signal, especially in salinity, while the model runs have a very pronounced eddy feature which adjusts the lower valued isohalines southward east of the eddy. As in the East China Sea, there are few differences in the modeled temperature and salinity between runs. The sgrid shows the largest differences from the other runs because the sgrid contain boundary errors that propagate upstream. Recall that the sgrid uses Orlanski radiation boundary conditions for u- and v-velocities instead of the advective scheme and zero velocity boundary conditions of the other runs. The radiation boundary conditions are known to produce errors that propagate back into the model domain (Durran, 2001; Kantha and Clayson, 2000).

The EKWC region contains the majority of the observations; the diamond on 01 March 2002, the triangle on 08 March 2002, the square on 29 March 2002, and the star on 29 March 2002. The EKWC is saltier and warmer than the general TWW. The depth of the thermocline at all of the EKWC locations is under-predicted. This is the result of the models being relaxed to the MODAS 3D temperature, which also strongly influences

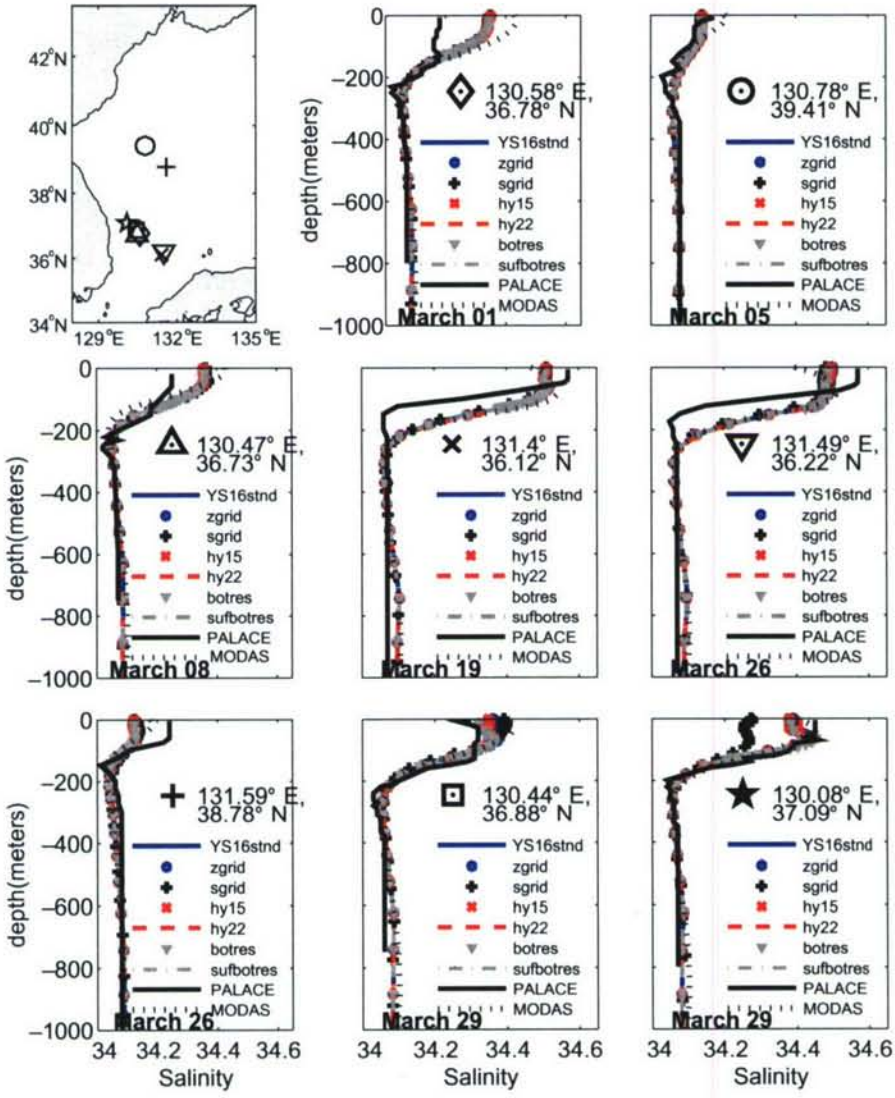

Fig. 10. Salinity profiles for the seven model runs, MODAS 3D, and PALACE float data.

the thermocline depth. The modeled salinity, again following the MODAS salinity, is saltier than the observations for all locations except the location represented by the star on 29 March 2002. At the star location, the MODAS salinity is close to the observations, but the model runs are influenced by the strong eddy. Again, the model runs show very similar temperature and salinity profiles. The exception being the sgrid at the star location on 29 March 2002. The sgrid is cooler and fresher here because it has a southward flowing current along the Korean coast while the rest of the runs have a northward flowing current.

The TWC region is represented by the "x" on 19 March 2002 and the inverted triangle on 26 March 2002. This region is the warmest and saltiest of the JES water mass regions shown. The model runs over estimate the thermocline and pycnocline depths. Once again they are following the MODAS forcing which appears to mix too strongly in this location. This region has some dynamic variability so the model runs are slightly different near the surface, but they all show similar trends.

The modeled salinity appears to have particular problems when compared to observations. The trend of the modeled salinity being fresher than the observations has also been observed in an Inter-American Seas (IAS) version of the NCOM run at NRL. The IAS model is a nowcast/forecast system that has been set-up to run operationally like global NCOM and the EAS16. The IAS also assimilates the 3D MODAS product which is tends be fresher than CTD observations (http://www7320.nrlssc.navy.mil/IAS_NFS/IASNFS_ctd.html).

4. Operational dynamic climatology – MODAS

Because of the bias in the salinity values in MODAS, it might seem curious that this assimilation is retained. To see the effect that MODAS has on the NCOM results, the seven previously discussed runs (Table 1) were rerun without the MODAS 3D or SST/SSS assimilation. Note that the initialization values and the boundary conditions still retain the influence of the original MODAS assimilation.

The MODAS assimilation has a positive overall influence on the NCOM results. This is demonstrated by looking at the Kuroshio front location (Fig. 11). The approximate Kuroshio front location is obtained from infrared satellite imagery maintained by NAVOCEANO as a front bogus. The model front location is along the 21.5 °C temperature contour (Hsueh et al., 1996; Lie et al., 1995). The 21.5 °C temperature contour of the YS16stnd run with MODAS assimilation matches the satellite frontal position better than the YS16stnd run without MODAS assimilation. In particular, the MODAS assimilation allows the model to better capture the location of the retroflection of the Kuroshio before it exits the East China Sea through the Tokara Strait.

The MODAS assimilation also contributes to the hybrid model runs similar results by reducing the variability between runs (Figs. 12 and 13). The NCOM model runs without MODAS assimilation are cooler and fresher than the NCOM runs with MODAS assimilation in the TWW region. The EKWC region shows similar temperature and salinity profiles with or without MODAS assimilation, but the end of March show a greater variability in the model solutions when there is no assimilation. The TWC region is also cooler and fresher in the no assimilation runs.

This shows that the MODAS assimilation is an important component of the NCOM operational system. The assimilation improves the model results and improves the robustness of the vertical grid design. The improvement to NCOM that MODAS provides has also been shown by Barron et al. (2005, 2006).

5. Conclusions

The seven different model runs of the YS16 domain produce very similar results for most of the domain. This can be attributed to the MODAS 3D product constraining the temperature and salinity and to the use of 1/16° grid resolution in the horizontal and 40 levels in the vertical being enough to resolve much of the circulation in this domain. This results in the RMS difference of the runs relative to the YS16stnd run (Table 2) being very small. The hy22 run is the most like the YS16stnd run and the sgrid is the most unlike the YS16stnd run. The botres case has large RMS differences in the temperature and salinity, which is expected because the first layer is at 15 m depth. The sgrid case has difficulty with the steep topography and contains propagating features that appear to be caused by the open boundary conditions. In particular, in the JES there is a southward flowing coastal current, which appears to be a coastally trapped wave, that originates at the eastern JES outflow boundary. It is thought that the trapped wave is a result of the boundary conditions used.

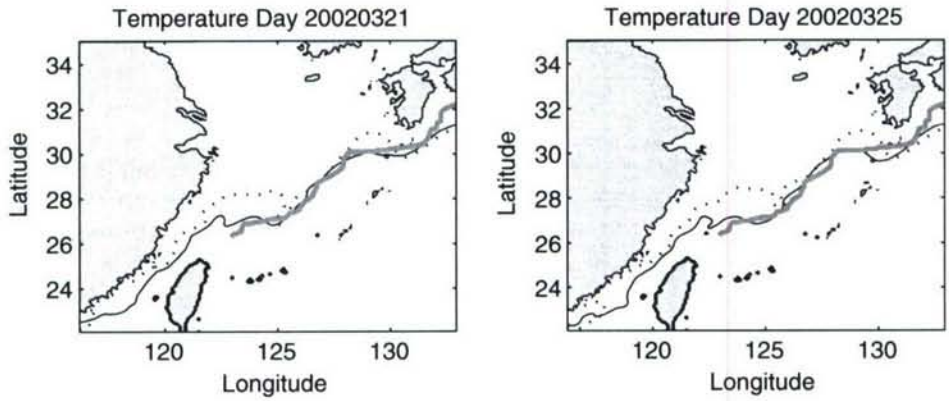

Fig. 11. Kuroshio front location (21.5 °C) given by NAVOCEANO front bogus (gray), YS16stnd with MODAS assimilation (black solid line), and YS16stnd without MODAS assimilation (black dotted line).

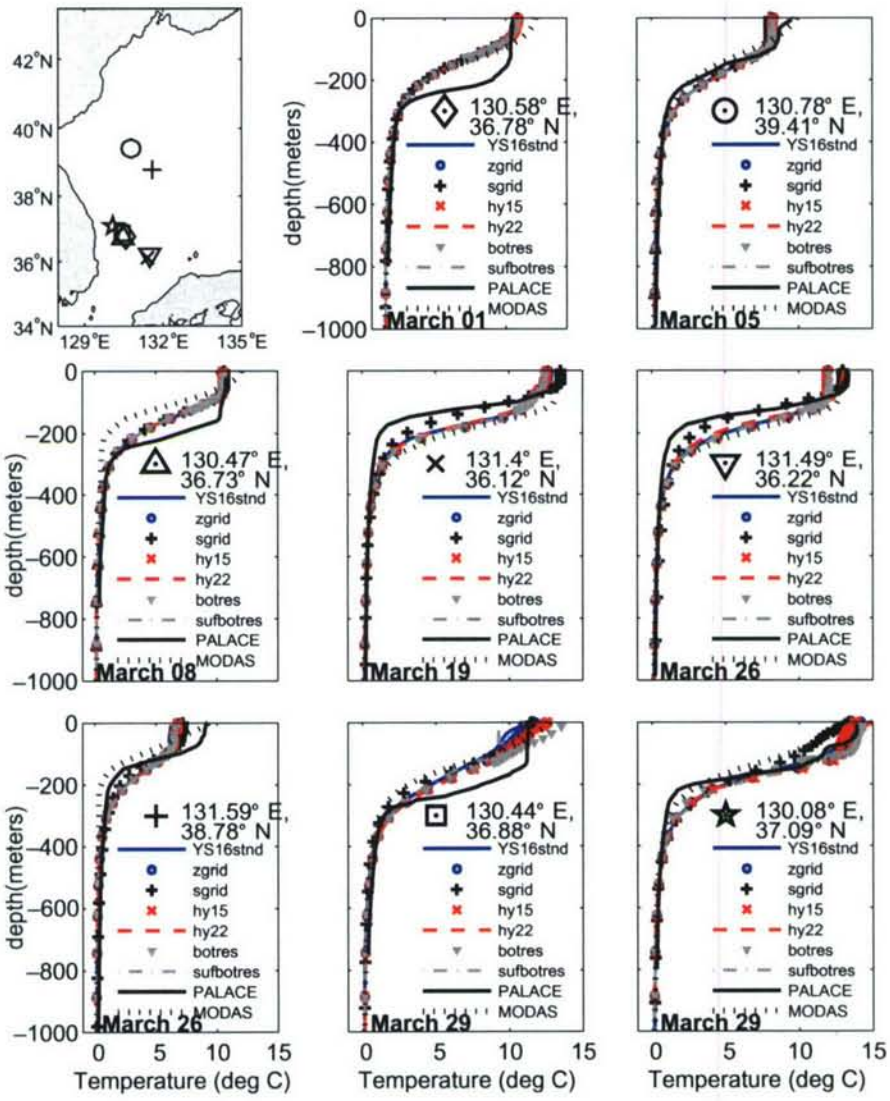

Fig. 12. Same as Fig. 9 but without MODAS assimilation.

The TS plots show that most of runs variability in the vertical is limited to above 400 m, which demonstrates the strength of the relaxation to the 3D MODAS field at depth. The YS16 runs' accuracy in modeling observed temperature and salinity is limited by the accuracy of the MODAS 3D product at any given time and location. This makes the real difference between runs the temperature and salinity values above 400 m and the calculated velocities. To test the accuracy of temperature and salinity of the different runs over the upper 400 m, RMS error per profile is calculated against 24 in situ profiles, which include the five previously discussed XBT's in the East China Sea and the eight PALACE floats in the Japan/East Sea plus ten additional PALACE floats in the Japan/East Sea and one additional float in the open Pacific at 132.87°E, 22.35°N (Table 3). The mean RMS errors show that overall the YS16stnd run does the best of the runs, but that any of the runs, with the exception of the sgrid run, would overall perform equally as well in this domain. The minimum RMS error of each profile shows another aspect of the model performance (Fig. 14). The sgrid has the minimum RMS error at 10 of the 24 profile locations, more than any other grid. Yet, the difficulty in quickly setting up a stable sigma coordinate model makes the sgrid configuration an undesirable choice for a rapidly relocatable model.

The comparison of observed to model drifter tracks (Fig. 7) in the ECS show that the YS16stnd vertical design, that is used in the 1/8° global NCOM and the 1/16° EAS16 nowcast/forecast runs, does a good job

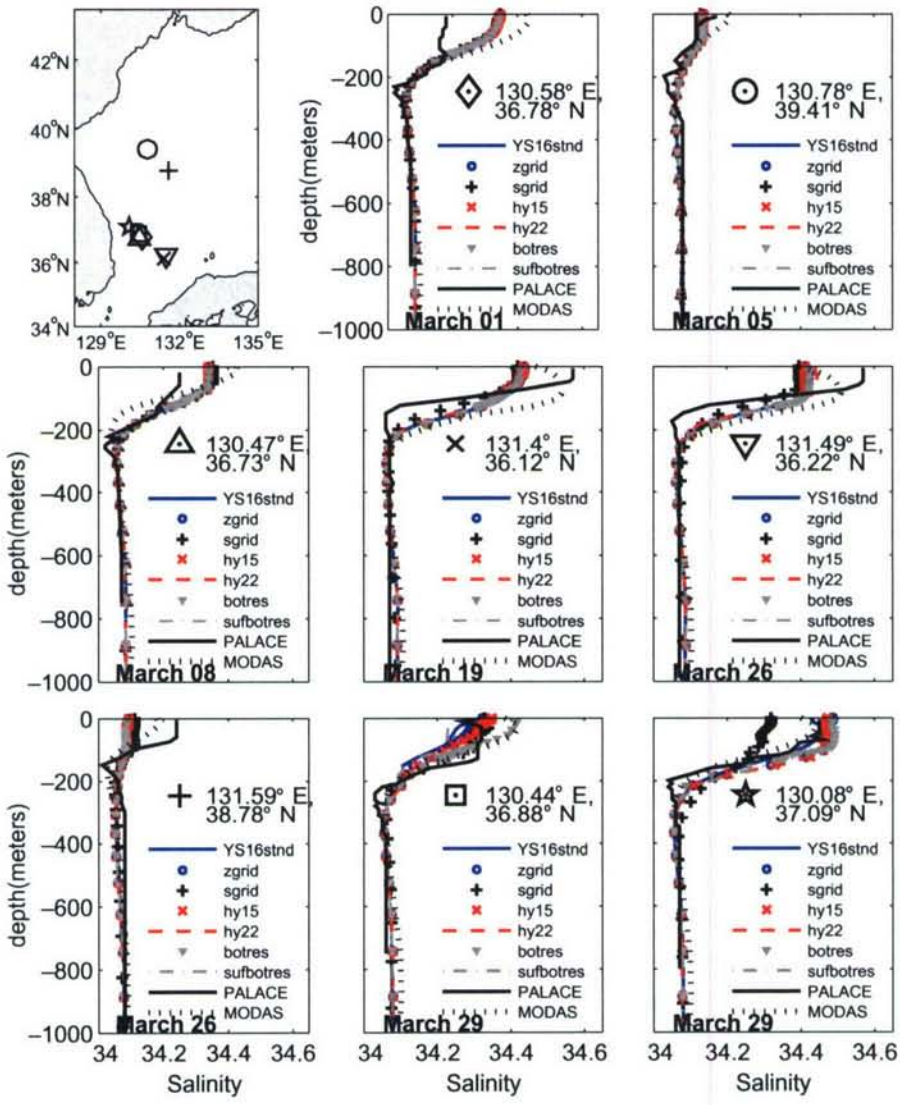

Fig. 13. Same as Fig. 10 but without MODAS assimilation.

Table 2
RMS difference for the YS16 model runs as compared to the YS16stnd run

Run name	*u*-Velocity (m/s)	*v*-Velocity (m/s)	Temperature (°C)	Sal (PSU)
zgrid	0.0110	0.0114	0.0646	0.0802
sgrid	0.0404	0.0441	0.2290	0.0652
hy15	0.0103	0.0105	0.0597	0.0499
hy22	0.0093	0.0095	0.0522	0.0354
botres	0.0199	0.0209	0.1825	0.7955
sufbotres	0.0097	0.0098	0.0598	0.0494

of reproducing the observations. The hy22 and sufbotres cases also do well. The hy22 case does particularly well in the ECS because it captures more of the shelf break area with sigma coordinates. The sufbotres case does particularly well in the ECS because of the high resolution in both the surface and near the bottom of the shelf.

Table 3
Mean RMS error for the YS16 model runs as compared to the upper 400 m of 19 CTD and 5 XBT profiles

Run name	Temperature (°C)	Sal (PSU)
YS16stnd	1.57	0.0586
zgrid	1.58	0.0590
sgrid	1.69	0.0607
hy15	1.58	0.0591
hy22	1.59	0.0589
sufbotres	1.58	0.0585

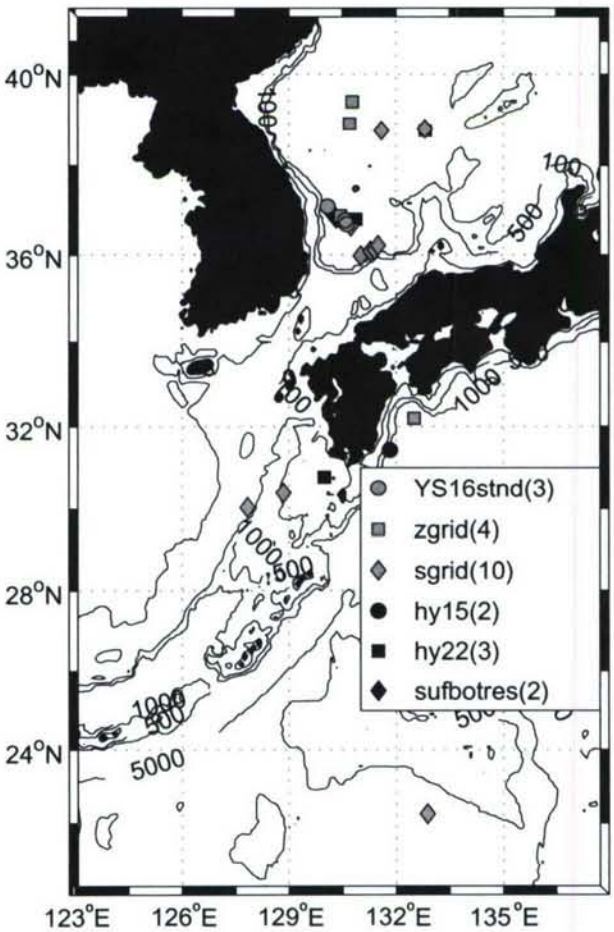

Fig. 14. Points showing the locations of 24 in situ profiles and the model with the minimum RMS error at each location.

It is harder to determine the success of the different runs in the YS and the JES without velocity observations. Overall, it can be said that the YS16stnd, zgrid, hy15, hy22, and sufbotres all give similar results. The botres case does not resolve the surface; therefore, it does not give good results in many locations. The sgrid has error associated with the open boundaries and the steep topography. These issues would need to be resolved before using a full sigma grid in this or any new domain, which would not make the sgrid a viable rapidly relocatable vertical grid choice.

It can be concluded that as long as the number of vertical levels used resolve the physics of the domain the NCOM hybrid model should give reasonable results. It appears that the best results occur when the transition depth from the sigma coordinates to z-levels occurs near the shelf break depth; therefore, for a rapidly relocatable NCOM system the YS16stnd grid is a good first choice for the vertical grid.

Acknowledgements

This research was conducted under a National Research Council Associateship: contract number N00173002-2-C005. We would like to thank Charlie Barron of NRL for supplying the code to calculate drifter trajectories from the NCOM model output. Thanks also to William J. Teague who provided insight into the observational data, and to Paul J. Martin who provided many suggestions throughout this research.

References

Barron, C.N., Kara, A.B., Hurlburt, H.E., Rowley, C., Smedstad, L.F., 2005. Sea surface height predictions from the Global Navy Coastal Ocean Model during 1998–2001. J. Tech. 21, 1876–1893.

Barron, C.N., Kara, A.B., Martin, P.J., Rhodes, R.C., Smedstad, L.F., 2006. Formulation, implementation and examination of vertical coordinate choices in the Global Navy Coastal Ocean Model (NCOM). Ocean Modell. 11, 347–375.

Barron, C.N., Kara, A.B., Rhodes, R.C., Rowley, C., Smedstad, L.F., 2006. Validation test report for the 1/8° Global Navy Coastal Ocean Model nowcast/forecast system. Nav. Res. Lab., Stennis Space Center, MS, NRL MR 7320-06-9019, 144 pp.

Bleck, R., 2002. An oceanic general circulation model framed in hybrid isopycnic–cartesian coordinates. Ocean Modell. 4, 55–88.

Candela, J., Beardsley, R.C., Limeburner, R., 1992. Separation of tidal and subtidal currents in ship-mounted acoustic doppler current profiler observations. J. Geophys. Res. 97 (C1), 769–788.

Chang, K.-I., Suk, M.-S., Pang, I.-C., Teague, W.J., 2000. Observations of the Cheju current. J. Korean Soc. Oceanogr. 35 (3), 129–152.

Chassignet, E.P., Arango, H., Dietrich, D., Ezer, T., Ghil, M., Haidvogel, D.B., Ma, C.-C., Mehra, A., Paiva, A.M., Sirkes, Z., 2000. DAMÉE-NAB: the base experiment. Dyn. Atmos. Oceans 32, 155–183.

Durran, D.R., 2001. Open boundary conditions: fact and fiction. In: Hodnett, P.F. (Ed.), IUTAM Symposium on Advances in Mathematical Modelling of Atmosphere and Ocean Dynamics. Kluwer Academic, Dordrecht, p. 118.

Fox, D.N., Teague, W.J., Barron, C.N., Carnes, M.R., Lee, C.M., 2002. The Modular Ocean Data Assimilation System (MODAS). J. Atmos. Ocean. Tech. 19 (2), 240–252.

Haidvogel, D.B., Beckmann, A., 1999. Numerical ocean circulation modeling. Series on Environmental Science and Management 2, IPC, 320 pp.

Halliwell, G.R., 2004. Evaluation of vertical coordinate and vertical mixing algorithms in the HYbrid-Coordinate Ocean Model (HYCOM). Ocean Modell. 7, 285–322.

Hansen, D.V., Poulain, P.M., 1996. Quality control and interpolations of WOCE–TOGA drifter data. J. Atmos. Ocean. Tech. 13 (4), 900–909.

Hogan, T.F., Brody, L.R., 1993. Sensitivity studies of the Navy Global Forecast Model parameterizations and evaluation of improvements to NOGAPS. Mon. Weather Rev. 121 (8), 2372–2395.

Hogan, T.F., Rosmond, T.E., 1991. The description of the Navy Operational Global Atmospheric Prediction System. Mon. Weather Rev. 119 (8), 1786–1815.

Hsueh, Y., Lie, H.-J., Ichikawa, H., 1996. On the branching of the Kuroshio west of Kyushu. J. Geophys. Res. 101 (C2), 3851–3857.

Hyatt, J., Signell, R.P., 1999. Modeling surface trapped river plumes: a sensitivity study. In: Spaulding, M.L., Butler, H.L. (Eds.), Estuarine and Coastal Modeling: Proceedings of the Sixth International Conference. ASCE, pp. 452–465.

Isoda, Y., Saitoh, S.-I., 1993. The northward intruding eddy along the East Coast of Korea. J. Oceanogr. 49, 443–458.

Kantha, L.H., Clayson, C.A., 2000. Numerical Models of Oceans and Oceanic Processes. Academic Press, San Diego, p. 940.

Lie, H.-J., Cho, C.-H., Lee, J.-H., Niiler, P., Hu, J.-H., 1995. Separation of the Kuroshio water and its penetration onto the continental shelf west of Kyushu. Int. WOCE Newslett. 20, 10–13.

Martin, P.J., 2000. A description of the Navy Coastal Ocean Model Version 1.0. NRL Report: NRL/FR/7322-00-9962, NRL, Stennis Space Center, MS, 39 pp.

Mellor, G.L., Häkkinen, S.M., Ezer, T., Patchen, R.C., 2002. A generalization of a Sigma Coordinate Ocean Model and an intercomparison of model vertical grids. In: Pinardi, N., Woods, J. (Eds.), Ocean Forecasting: Conceptual Basis and Applications. Springer, pp. 55–72.

Niiler, P.P., 2001. The world ocean surface circulation. In: Siedler, G., Church, J., Gould, J. (Eds.), Ocean Circulation and Climate. Academic Press, pp. 193–203.

Preller, R.H., Hogan, P.J., 1998. Oceanography of the Sea of Okhotsk and the Japan/East Sea. In: Robinson, A., Brink, K. (Eds.), The Sea: The Global Coastal Ocean. John Wiley and Sons, pp. 429–481.

Rosmond, T.E., 1992. The design and testing of the Navy Operational Global Atmospheric Prediction System. Weather Forecast. 7 (2), 262–272.

Teague, W.J., Carron, M.J., Hogan, P.J., 1990. A comparison between the Generalized Digital Environmental Model and Levitus Climatologies. J. Geophys. Res. 95 (C5), 7167–7183.

Willebrand, J., Barnier, B., Böning, C., Dieterich, C., Killworth, P.D., Le Provost, C., Jia, Y., Molines, J.-M., New, A.L., 2001. Circulation characteristics in three eddy-permitting models of the North Atlantic. Prog. Oceanogr. 48, 123–161.